

Communication

Management of Exciton Distribution for High-Performance Organic Light-Emitting Diodes Based on Interfacial Exciplex Architecture

Ren Sheng ^{1,†}, Cong Chen ^{1,†}, Erdong Zhang ¹, Wencheng Zhao ¹, Jihua Tang ¹, Duxu Yan ¹, Zhengze Li ² and Ping Chen ^{1,*}

¹ Institute of Physics and Electronic Information, Yantai University, Yantai 264005, China; rensheng@ytu.edu.cn (R.S.); congchen@s.ytu.edu.cn (C.C.); erdongzhang@s.ytu.edu.cn (E.Z.); 18265892850@163.com (W.Z.); fanhuokua111@126.com (J.T.); yandx316@s.ytu.edu.cn (D.Y.)

² State Key Laboratory on Integrated Optoelectronics, College of Electronic Science & Engineering, Jilin University, Changchun 130012, China; 13091682837@163.com

* Correspondence: pingchen@jlu.edu.cn; Tel.: +86-1360-431-2567

[†] These authors contributed equally to this work.

Abstract: Interfacial exciplex has recently been adopted as an effective host to achieve phosphorescent organic light-emitting diodes (OLEDs) with high efficiencies and low driving voltages. However, a systematic understanding of exciton recombination behavior in either host of interfacial exciplex is still deficient. Herein, the strategic design rule of interfacial exciplex host is proposed to overcome the negative effects of direct trapping recombination by systematically investigating exciton recombination behavior in interfacial exciplex hosts. As a result, blue and orange phosphorescent devices acquire peak external quantum efficiencies of 23.5% and 29.2% with low turn-on voltages. These results provide a simple method to realize highly efficient OLEDs aiming for general lighting and display applications.

Keywords: organic light-emitting diodes; exciplex; phosphorescence; high efficiency



Citation: Sheng, R.; Chen, C.; Zhang, E.; Zhao, W.; Tang, J.; Yan, D.; Li, Z.; Chen, P. Management of Exciton Distribution for High-Performance Organic Light-Emitting Diodes Based on Interfacial Exciplex Architecture. *Molecules* **2023**, *28*, 7028. <https://doi.org/10.3390/molecules28207028>

Academic Editor: Roy Man-Keung Fung

Received: 28 August 2023

Revised: 30 September 2023

Accepted: 3 October 2023

Published: 11 October 2023



Copyright: © 2023 by the authors. Licensee MDPI, Basel, Switzerland. This article is an open access article distributed under the terms and conditions of the Creative Commons Attribution (CC BY) license (<https://creativecommons.org/licenses/by/4.0/>).

1. Introduction

Organic light-emitting diodes (OLEDs) hold great promise for applications in full-color display and solid-state lighting because of their striking advantages, such as high efficiency, fast response, and flexibility [1–4]. In order to pursue high efficiency, phosphor-doped OLEDs are a highly effective approach because of 100% internal quantum efficiency in principle via harnessing both singlet and triplet excitons [5–7]. Generally, phosphorescent dyes are used as the guest and doped into the host matrix to realize a high performance of energy transfer system [8,9]. Consequently, the performance of devices is mainly determined by the properties of the host materials, which may act as the main charge transport channels and recombination centers, resulting in increased limitations in fabrication [10–13].

Recently, the exciplex system co-doped between the donor and acceptor is considered a promising technology to overcome the above barriers [14–17]. Owing to the intrinsically small energy gap (ΔE_{ST}) between the triplet level (T_1) and singlet level (S_1), triplet excitons could be upconverted into singlet by efficient reverse intersystem crossing (RISC) process [18–20]. This efficient upconversion provides markedly enhanced long-range dipole–dipole coupling (Förster energy transfer) from the exciplex host to dopants, leading to high-efficiency OLEDs under low doping levels [21,22]. However, the co-evaporation of mixed host materials with dopant significantly aggravates the complexity of the manufacturing process, obstructing the large-scale commercialization application.

To settle this problem, interfacial exciplex is exploited as a host for achieving high-performance OLEDs with an uncomplicated fabrication process [23,24]. By employing

bilayer exciplex architecture, charge-transfer (CT) excitons could be formed between the donor and acceptor at the heterointerface conspicuously with the suppressed formation of the donor excited states, leading to an efficient energy transfer from host to guest [24]. Recently, Wu et al. demonstrated orange OLED with a high external quantum efficiency (EQE) of 14.3% and suppressed roll-off by combining an ultrathin phosphor layer and interfacial exciplex host [25]. Wang et al. reported efficient interfacial-exciplex-hosted red phosphorescent OLED with maximum power efficiency (PE) of 40.4 lm W⁻¹ by solution-processing method [26]. However, the systematic investigation of the EL mechanism in either host of interfacial exciplex has not yet been demonstrated, and OLED based on an interfacial exciplex system with outstanding efficiency is scarcely reported so far.

In this work, the influence of exciton recombination behavior in interfacial exciplex hosts on the performance of the device is investigated, indicating suppressed charge trapping and efficient Förster energy transfer from interface exciplex to the guests are the key factors for improving the performance of interfacial exciplex hosted devices. By doping phosphorescent dyes into the acceptor host of interface exciplex structure constructed by the donor of 2,6-bis(3-(carbazol-9-yl)phenyl)pyridine (26DCzPPy) and the acceptor of 4,6-bis[3,5-(dipyrid-3-yl)-phenyl]-2-phenylpyrimidine (B4PyPPM), highly efficient blue and orange phosphorescent OLEDs with maximum EQEs of 23.5% and 29.2% are provided, which is one of the best values in OLEDs based on simplified architectures.

2. Results

As for common phosphorescent OLEDs, hole-dominated or bipolar organic materials are frequently used as hosts for dopants according to the design principle of charge balance [27–29]. As depicted in Figure 1a, the highest occupied molecular orbital (HOMO) levels of the hosts are substantially below the HOMO of the dopants due to the smaller band gap of dopants; thus, the dopants are expected to trap holes. On the other hand, electrons could transport to the lowest unoccupied molecular orbital (LUMO) of hosts, easily arising from a minor energy gap between the electron-transport layers and hosts. These electrons are further trapped by dopants, leading to dominated trap-assisted charge recombination on dopant molecules. While referring to donor-hosted devices based on interfacial exciplex, as shown in Figure 1b, owing to large HOMO-LUMO offset between donor and acceptor, electrons accumulated at the heterointerface prefer to overcome barriers and inject into the dopants rather than donor molecules, causing increased operation voltage. Specifically, the charge trapping effect would hinder the transport of holes inside the emission layers; therefore, holes could barely reach the heterointerface, resulting in the significantly suppressed formation of CT excitons. In such cases, efficient energy transfer from exciplex host to guest is dramatically restrained, which is the main reason for poor EL performance of the devices with interfacial exciplex host. In contrast, by using acceptors as hosts, the trap-assisted recombination on dopants could be suppressed, as shown in Figure 1c. Thanks to the LUMO energy barrier between acceptor molecules and dopants, electrons would pass through the acceptor layer along the LUMO of the acceptor predominantly without a trapping effect. Note that CT excitons could be effectively formed by interfacial molecular interactions between donor and acceptor. Accordingly, it is possible that the energy of the CT excitons would be transferred to the dopants efficiently, leading to superior device performance.

To demonstrate the influence of different operating mechanisms on device performance, two groups of devices are fabricated based on the interfacial exciplex formed by 26DcZPPy and B4PyPPM with the structure of ITO/HAT-CN (10 nm)/TAPC (35 nm)/TCTA (5 nm)/26DcZPPy (5 nm)/emission layer (20 nm)/B4PyPPM (35 nm)/Liq (0.8 nm)/Al. Here, the emission layers are 26DCzPPy: 10%FIrPic; 26DCzPPy: 3%PO-01; B4PyPPM: 10%FIrPic; and B4PyPPM: 3%PO-01, corresponding to device B₁, O₁, B₂ and O₂, respectively. Figure 2a,b exhibit the detailed energy level diagram and the molecule structures of required materials, respectively. The formation of exciplex could be demonstrated by the red-shift PL spectrum of mixed film compared with those of constituting molecules

and TADF characteristics in transient PL decayed curves in Figure S1 [30]. The exciplex of 26DCzPPy: B4PyPPM possesses a minor ΔE_{ST} of 35 meV and an efficient RISC process, which are beneficial for preparing efficient OLEDs [31]. Figure 3a,b show the current efficiency (CE) and PE curves of four devices. Device B₁ and device O₁ only give maximum efficiencies of 16.7 lm W⁻¹ (24.3 cd A⁻¹) and 26.6 lm W⁻¹ (45.3 cd A⁻¹), respectively, whereas it is found that ultra-high efficiencies are realized as the dopants are doped in B4PyPPM, displaying high PEs of 36.7 lm W⁻¹ for device B₂ and 78.9 lm W⁻¹ for device O₂, which is 2.2 folds higher than that of device B₁ and 2.9 folds higher than that of device O₁, respectively. Additionally, devices B₂ and O₂ show low turn-on voltages of 2.6 V and 2.4 V despite large charge injection barriers between 26DcZPPy and B4PyPPM, which are significantly reduced compared to 3.8 V for device B₁ and 4.2 V for O₁. It can be considered that the properties of host materials greatly affect the EL performance of devices. Despite the bipolar transport property of 26DcZPPy, B4PyPPM is adequately demonstrated to be the host for emitting dyes in our interface exciplex system. It is generally agreed that the charge transport pathway is a typical behavior to estimate the emission mechanism of the devices [32]. As can be seen in Figure 3c,d, current densities show a strong dependence on dopants in 26DCzPPy hosted devices, which have little effect on current densities in B4PyPPM hosted devices. These phenomena possibly indicate that trap-assisted recombination plays an important role in the EL process of the devices with 26DCzPPy host, which is suppressed in the devices with B4PyPPM host. To further understand the emission mechanism, transient EL decay curves are further carried out. As shown in Figure 4, transient overshoots in the turn-off region are observed in devices O₁ and B₁ with the 26DcZPPy-hosted structure, which can be attributed to charge carrier trapping in the dopants [33]. However, overshoots are barely observed in devices O₂ and B₂. This phenomenon demonstrates that accumulated charge carriers are released and recombined after bias turn-off in devices O₁ and B₁, which may also cause longer decay time in devices O₁ and B₁ compared to those in devices O₂ and B₂.

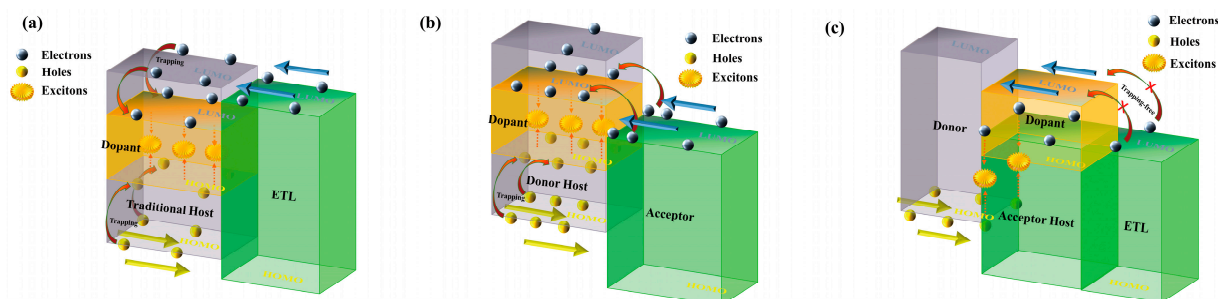


Figure 1. The operational mechanism of devices based on (a) traditional host, (b) donor host, and (c) acceptor host.

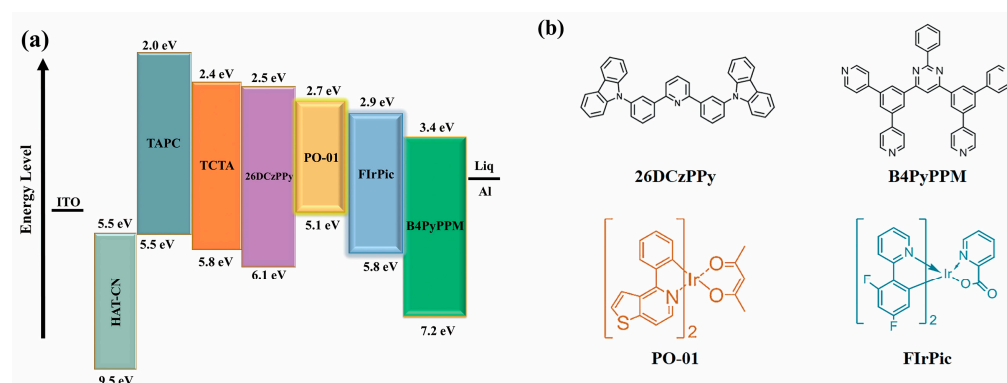


Figure 2. (a) The detailed energy level diagram of the used materials. (b) The molecular structures of the materials used in this work.

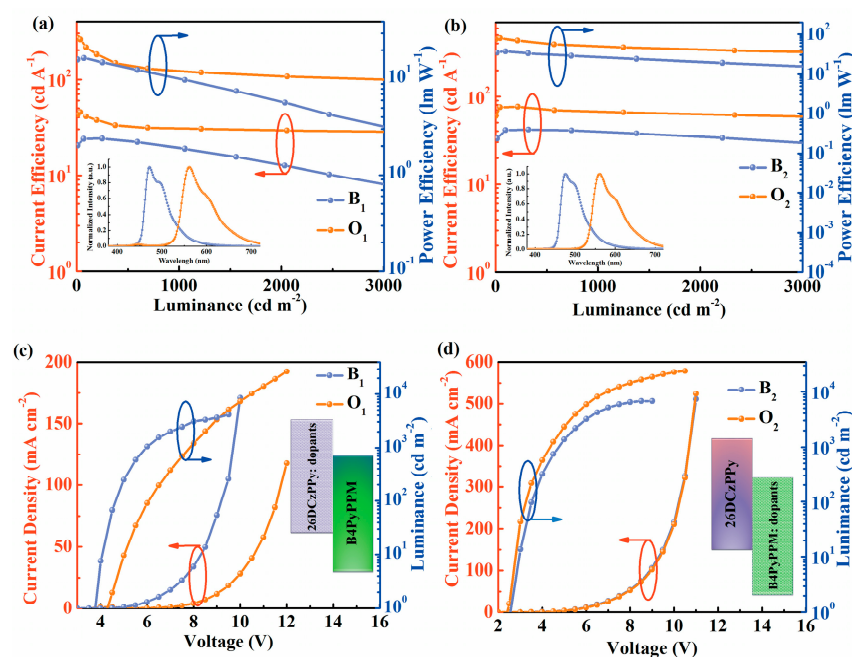


Figure 3. The current efficiency–luminance–power efficiency characteristics of devices (a) B₁–O₁ and (b) B₂–O₂. Inserts: normalized EL spectra of the devices at 5 V. The current density–voltage–luminance characteristics of devices (c) B₁–O₁ and (d) B₂–O₂.

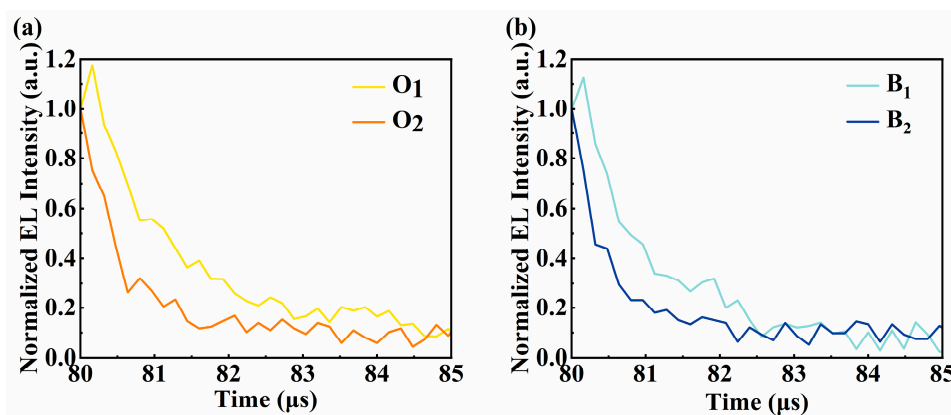


Figure 4. The transient EL decay of (a) devices O₁ and O₂ and (b) devices B₁ and B₂.

To further demonstrate the influence of dopants on charge transport properties in devices with interfacial exciplex host, single-carrier devices are carried out successively with the structure of ITO/HAT-CN (10 nm)/TAPC (35 nm)/TCTA (5 nm)/26DcZPPy (5 nm)/26DCzPPy: 10%FIrPic or 3%PO-01 (20 nm)/TAPC (35 nm)/HAT-CN (10 nm)/Al and ITO/Liq (0.8 nm)/B4PyPPM (35 nm)/B4PyPPM: 10%FIrPic or 3%PO-01 (20 nm)/B4PyPPM (35 nm)/Liq (0.8 nm)/Al. Figure 5a,b show the single-carrier current density–voltage characteristics of 26DcZPPy hosted devices. It is important to confirm that doped devices exhibit significantly decreased hole current densities compared to that of the non-doped device, suggesting the dopants may act as charge trapping centers for holes due to the shallower HOMO levels of dopants than that of 26DcZPPy. Nevertheless, the electron current densities of doped devices show huge enhancements compared to the doping-free device, which can be explained by the fact that electrons transported from the B4PyPPM layer preferably inject into the LUMO levels of dopants assigned to their deeper LUMO levels compared to that of 26DCzPPy, which could facilitate electron transport into the emission layer. The higher electron current in the FIrPic-doped device than in PO-01 is attributed to the deeper LUMO and dominant electron transport property of FIrPic molecules. Figure 5c,d show the single carrier current

density–voltage characteristics of B4PyPPM-hosted devices. Obviously, there is no remarkable change in hole and electron current between doped and doping-free devices, indicating that dopants show barely any impact on both hole and electron transport, which is consistent with the above results.

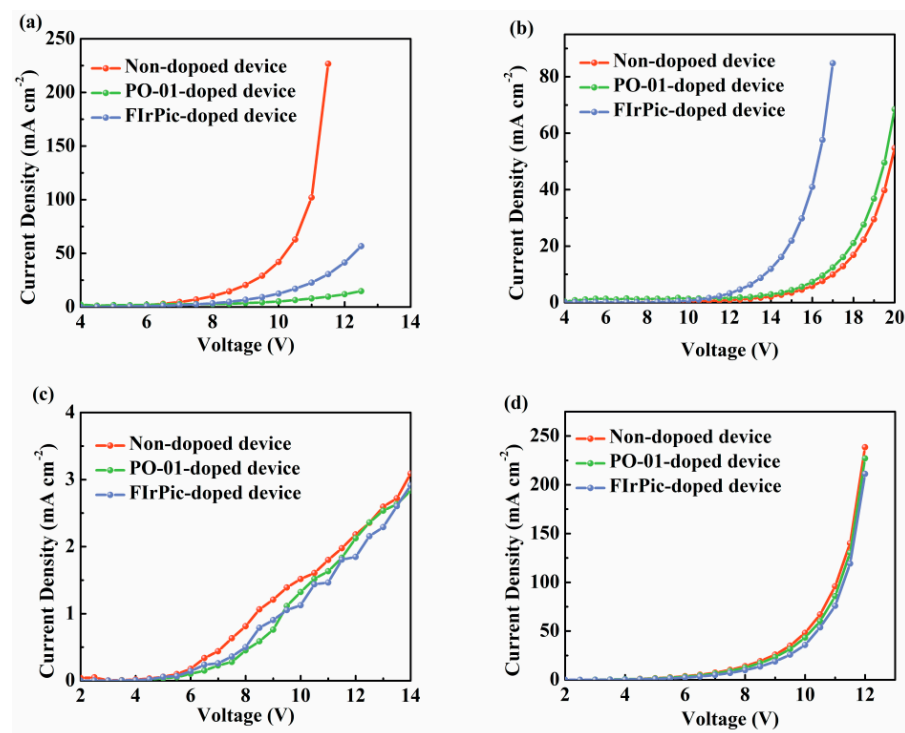


Figure 5. The current density–voltage characteristics of (a) hole- and (b) electron-only devices based on 26DcZPPy hosted devices. The current density–voltage characteristics of (c) hole- and (d) electron-only devices based on B4PyPPM hosted devices.

To better comprehend the two types of emission mechanisms, neat spacer layers with different thicknesses are inserted at the 26DcZPPy/B4PyPPM heterointerface in devices based on 26DcZPPy and B4PyPPM hosts, respectively. The emission layer structures of the devices are shown in the insets of Figure 6. The normalized EL spectra of 26DcZPPy hosted devices are shown in Figure 6a,b. All the spectra exhibit major dopant emission along with faint exciplex emission, suggesting the exciplex formation is suppressed at the interface of 26DcZPPy/B4PyPPM due to the hole-trapping effect in the 26DcZPPy host. As a result, the exciton recombination region should be sited in the doped emission layer, which deviates far from the interface of 26DcZPPy/B4PyPPM, leading to the restrained formation of interface exciplex. By contrast, for B4PyPPM hosted devices, holes injected from the anode can easily cross the transport layer and accumulate at the 26DcZPPy/B4PyPPM heterointerface, contributing to the large HOMO offset of 1.1 eV between 26DcZPPy and B4PyPPM as well as inferior hole transport property of B4PyPPM. On the other hand, because of the much deeper LUMO of B4PyPPM than that of dopants, electrons trapped by dopant molecules can be negligible. In this case, electrons injected from the cathode can reach the heterointerface without limitation, increasing the generation probability of exciplex-type excitons. Figure 6c,d exhibits the normalized EL spectra of B4PyPPM-hosted devices. As x is less than 5 nm, the interface exciplex generated by interfacial molecular interactions transfers the energy to the dopants effectively, leading to serious quenching of exciplex emission. With the further increasing thickness of the spacer, the blue emission from exciplex increases quickly, indicating energy transfer from exciplex to dopant become less efficient due to the separation between the doped layer and exciton recombination region. It is notable that strong dopant emission can be obtained in B4PyPPM hosted devices even with 10 nm spacers, as shown in Figure 6c,d, suggesting Förster energy

transfer could be identified as the main energy transfer channel since the Dexter energy transfer radius is estimated to be 1 nm.

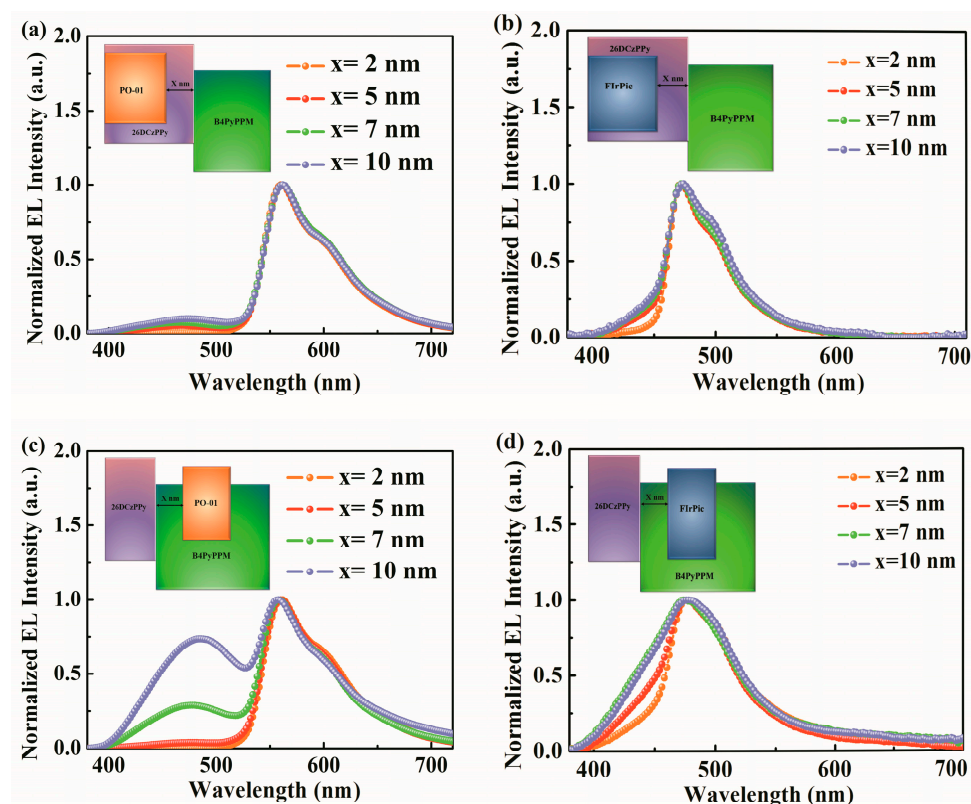


Figure 6. The normalized EL spectra of devices based on the emission layer of (a) 26DCzPPy: 3%PO-01, (b) 26DCzPPy: 10%FlrPic, (c) B4PyPPM: 3%PO-01, and (d) B4PyPPM: 10%FlrPic at 8 V.

To further optimize the performance of the blue and orange devices based on B4PyPPM hosted structure, the devices are fabricated by modulating doping concentration with the structure of ITO/HAT-CN (10 nm)/TAPC (35 nm)/TCTA (5 nm)/26DcZPPy (5 nm)/emission layer (20 nm)/B4PyPPM (35 nm)/Liq (0.8 nm)/Al. Here, the emission layers are B4PyPPM: 8%FlrPic, B4PyPPM: 12%FlrPic, B4PyPPM: 15%FlrPic, B4PyPPM: 1%PO-01, B4PyPPM: 4%PO-01 and B4PyPPM: 6%PO-01, corresponding to device B₄, B₅, B₆, O₄, O₅ and O₆, respectively. As shown in Figure 7a,b, the current density shows a slight variation as the doping concentration rises in both blue and orange devices, demonstrating charge trapping effects can be negligible. It is notable that device B₆ with 15% FlrPic and O₆ with 6% PO-01 show low turn-on voltages of 2.6 V and 2.3 V, which are close to the optical energy gaps of their molecules, suggesting the barrier-free exciton recombination in two devices. With the doping level increasing, efficiencies of blue and orange series devices enhance obviously, as shown in Figure 7c,d and Table 1. The maximum PEs of 45.9 lm W⁻¹ and 125.9 lm W⁻¹ are achieved in devices B₆ and O₆, respectively, which are one of the best reported phosphorescent OLEDs as shown in Table 2. Remarkably, even suffering low doping levels in devices B₄ and O₄, the energy of exciplex excitons can be harvested by dopants via Förster energy transfer effectively, performing high PEs of 33.6 lm W⁻¹ for device B₄ and 77.9 lm W⁻¹ for device O₄ with undetectable exciplex emission.

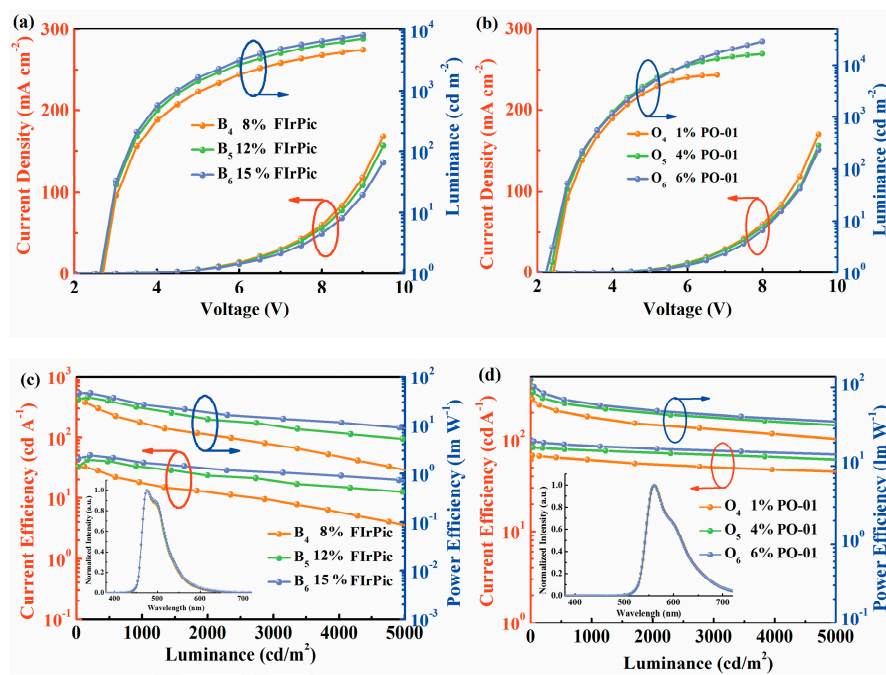


Figure 7. The current density-voltage-luminance characteristics of (a) B₄–B₆ and (b) O₄–O₆. The current efficiency-luminance-power efficiency characteristics of (c) B₄–B₆ and (d) O₄–O₆ inserts show normalized EL spectra of the devices at 5 V.

Table 1. EL Performance of orange and blue OLEDs.

	V _{on}	CE(cd/A) _{max/100/1000}	PE(lm/W) _{max/100/1000}	EQE(%) _{max/100/1000}	CIE
Device B ₃	2.7	38.7/33.9/30.4	38.9/25.7/16.7	18.0/15.8/14.2	(0.16, 0.36)
Device B ₄	2.7	33.0/32.6/17.8	33.6/32.1/11.2	15.3/15.1/8.3	(0.15, 0.36)
Device B ₅	2.6	42.6/37.7/34.0	38.2/36.0/22.8	19.8/17.5/15.8	(0.15, 0.36)
Device B ₆	2.6	50.6/45.7/37.7	45.9/45.4/28.2	23.5/21.2/17.5	(0.15, 0.36)
Device O ₃	2.7	92.2/90.8/83.9	87.7/77.8/51.6	26.9/26.4/24.5	(0.49, 0.50)
Device O ₄	2.4	67.6/59.8/50.0	77.9/66.3/40.5	20.5/17.6/15.1	(0.49, 0.50)
Device O ₅	2.3	85.2/77.7/69.2	107.1/84.3/56.3	24.9/22.7/20.2	(0.49, 0.50)
Device O ₆	2.3	100.2/86.0/76.1	125.9/96.9/61.6	29.2/25.1/22.2	(0.49, 0.50)

V_{on}: Turn-on voltages of the devices. CE_{max/100/1000}: the maximum CE/CE at 100 cd m⁻²/CE at 1000 cd m⁻². PE_{max/100/1000}: the maximum PE/PE at 100 cd m⁻²/PE at 1000 cd m⁻². EQE_{max/100/1000}: the maximum EQE/EQE at 100 cd m⁻²/EQE at 1000 cd m⁻². CIE: CIE coordinates at 1000 cd m⁻². Oversight.

Table 2. Summary of EL performance of phosphorescent OLEDs.

		V _{on}	PE _{max}	CE _{max}	EQE _{max}
Orange OLEDs	O ₆	2.3	125.9	100.2	29.2
	Ref [25]	3.6	37.4	40.5	14.3
	Ref [34]	3.0	79.4	80.9	26.1
	Ref [32]	2.5	57.6	50.7	18.5
	Ref [35]	2.5	74.1	59.0	20.4
Blue OLEDs	B ₆	2.6	45.9	50.6	23.5
	Ref [36]	2.9	44.7	42.5	-
	Ref [37]	3.0	30.9	32.6	16.0
	Ref [18]	2.6	47.4	40.7	20.1
	Ref [38]	2.62	27.30	29.24	-
	Ref [39]	2.4	66.0	-	30.3

V_{on}: Turn-on voltages of the devices. CE_{max}: the maximum CE. PE_{max}: the maximum PE. EQE_{max}: the maximum EQE.

Subsequently, for a comparison, blue and orange devices based on 26DcZPPy: B4PyPPM (1:1) co-doped exciplex host are designed, corresponding to device B₃ and O₃, respectively. Detailed EL characteristics are shown in Table 1 and Figure S2. The maximum PEs of the two devices are 38.9 lm W⁻¹ for device B₃ and 87.7 lm W⁻¹ for device O₃, which are lower than those of devices B₆ and O₆ but significantly better than devices B₁ and O₁. It is reasonable that energy transfer between exciplex and dopants should be effective in these devices, whereas the negative effects assigned to non-ignorable charge trapping are still inevitable during the transport process in the emission layer, which results in degradation of device performance.

3. Experimental Section

All the devices were fabricated on pre-patterned indium tin oxide (ITO) coated glass, and the sheet resistance of the transparent anode was 20 Ω/square. The ITO substrate was scrubbed sequentially with acetone, ethanol, and deionized water and cleaned in a UV ozone chamber for 5 min before being loaded into a high vacuum thermal system. An amount of 10 nm of 8-hydroxyquinolinolato-lithium (HAT-CN) was used as a hole injection layer. An amount of 1,1-Bis[(di-4-tolylamino)phenyl]cyclohexane (TAPC) and Tris(4-carbazoyl-9-ylphenyl)amine (TCTA) with high hole mobility were used as the hole transport layer and electron blocking layer, respectively. Additionally, 26DCzPPy and B4PyPPM were used as donors and acceptors of the interfacial exciplex, respectively. Bis(4-phenylthieno[3,2-c]pyridinato-N,C2') acetylacetonate iridium(III) (PO-01) and Bis[2-(4,6-difluorophenyl)pyridinato-C2,N](picolinato)iridium(III) (FlrPic) were used as orange and blue phosphorescent emission dyes, respectively. An amount of 0.8 nm Liq and 100 nm Al were deposited sequentially as cathodes. All the devices were fabricated in a high vacuum (5×10^{-4} Pa) thermal evaporation chamber. Organic layers were grown at the rate of 0.1–0.2 nm/s, while PO-01, FlrPic, and Liq were deposited at the rate of 0.02–0.08 Å/s, and Al cathode was deposited at the rate of 0.5 nm/s. Electroluminescence (EL) information of the devices was simultaneously measured using a PR655 spectro-scan spectrometer. The current-voltage and luminance-voltage characteristics were recorded by combining the spectrometer with a programmable Keithley 2450 voltage-current source.

4. Conclusions

In summary, highly efficient phosphorescent OLEDs based on simplified architecture are successfully achieved by employing an interface exciplex system constructed by 26DcZPPy and B4PyPPM. The resulting blue and orange phosphorescent OLEDs show maximum EQEs of 23.5% and 29.2% with low turn-on voltages. By investigating exciton recombination behavior in control devices, superior performance can be attributed to the efficient Förster energy transfer and suppressed charge carriers trapping effect via interface exciplex system. We believe that this design concept can provide a promising method for developing highly efficient OLEDs with simplified configurations.

Supplementary Materials: The following supporting information can be downloaded at: <https://www.mdpi.com/article/10.3390/molecules28207028/s1>. Figure S1. (a) The normalized PL spectra of 26DCzPPy, B4PyPPM and 26DCzPPy: B4PyPPM mixed film and the normalized EL spectra of 26DCzPPy: B4PyPPM 26DCzPPy/B4PyPPM bilayer devices. (b) The transient PL decay of 26DCzPPy: B4PyPPM mixed film measured at 300 K. Figure S2. The current density-voltage-luminance characteristics of (a) blue and (b) orange co-host devices. The current efficiency-luminance-power efficiency characteristics of (c) blue and (d) orange co-host devices.

Author Contributions: R.S. conceived and designed the experiments and wrote the original draft. C.C. and E.Z. performed the experiments and analyzed the data. W.Z., J.T., D.Y. and Z.L. provided some significant technical guidance. P.C. was involved in the interpretation of the results. All authors have read and agreed to the published version of the manuscript.

Funding: This research was funded by the National Natural Science Foundation of China (62205281) and the Taishan Scholars Plan of Shandong Province (tsqn201909084).

Institutional Review Board Statement: Not applicable.

Informed Consent Statement: Not applicable.

Data Availability Statement: Not applicable.

Conflicts of Interest: The authors declare no conflict of interest.

Sample Availability: Not applicable.

References

1. Lee, J.; Chen, H.F.; Batagoda, T.; Coburn, C.; Djurovich, P.I.; Thompson, M.E.; Forrest, S.R. Deep blue phosphorescent organic light-emitting diodes with very high brightness and efficiency. *Nat. Mater.* **2016**, *15*, 92–98.
2. Li, H.Y.; Zhou, L.; Teng, M.Y.; Xu, Q.L.; Lin, C.; Zheng, Y.X.; Zuo, J.L.; Zhang, H.J.; You, X.Z. Highly efficient green phosphorescent OLEDs based on a novel iridium complex. *J. Mater. Chem. C* **2013**, *1*, 560–565.
3. Wang, Q.; Ma, D. Management of charges and excitons for high-performance white organic light-emitting diodes. *Chem. Soc. Rev.* **2010**, *39*, 2387–2398.
4. Ying, L.; Ho, C.L.; Wu, H.; Cao, Y.; Wong, W.Y. White polymer light-emitting devices for solid-state lighting: Materials, devices, and recent progress. *Adv. Mater.* **2014**, *26*, 2459–2473.
5. Schwartz, G.; Pfeiffer, M.; Reineke, S.; Walzer, K.; Leo, K. Harvesting triplet excitons from fluorescent blue emitters in white organic light-emitting diodes. *Adv. Mater.* **2007**, *19*, 3672–3676.
6. Fukagawa, H.; Shimizu, T.; Osada, Y.; Kamada, T.; Kiribayashi, Y.; Yamamoto, T.; Shimidzu, N. Direct Observation of Efficient Triplet–Triplet Energy Transfer in Phosphorescent Organic Light-Emitting Diode. *Appl. Phys. Express* **2013**, *6*, 052104. [[CrossRef](#)]
7. Chen, P.; Sheng, R.; Ko, M.Y.; Duan, Y.; Cheng, G.; Che, C.M. Efficient white organic light-emitting diodes with double co-host emitting layers. *J. Mater. Chem. C* **2018**, *6*, 9890–9896.
8. Ho, C.L.; Lin, M.F.; Wong, W.Y.; Wong, W.K.; Chen, C.H. High-efficiency and color-stable white organic light-emitting devices based on sky blue electrofluorescence and orange electrophosphorescence. *Appl. Phys. Lett.* **2008**, *92*, 083301. [[CrossRef](#)]
9. Liu, X.K.; Zheng, C.J.; Lo, M.F.; Xiao, J.; Chen, Z.; Liu, C.L.; Lee, C.S.; Fung, M.K.; Zhang, X.H. Novel blue fluorophor with high triplet energy level for high performance single-emitting-layer fluorescence and phosphorescence hybrid white organic light-emitting diodes. *Chem. Mater.* **2013**, *25*, 4454–4459. [[CrossRef](#)]
10. Ma, W.; Zhao, W.; Chen, C.; Zhang, E.; Tang, J.; Yan, D.; Sun, Y.; Chen, P.; Sheng, R. Highly efficient fluorescent organic electroluminescent diodes based on doping-free phosphorescent sensitization system. *Org. Electron.* **2023**, *116*, 106772. [[CrossRef](#)]
11. Pan, B.; Wang, B.; Wang, Y.; Xu, P.; Wang, L.; Chen, J.; Ma, D. A simple carbazole-N-benzimidazole bipolar host material for highly efficient blue and single layer white phosphorescent organic light-emitting diodes. *J. Mater. Chem. C* **2014**, *2*, 2466–2469. [[CrossRef](#)]
12. Liu, B.; Wang, L.; Gao, D.; Xu, M.; Zhu, X.; Zou, J.; Lan, L.; Ning, H.; Peng, J.; Cao, Y. Harnessing charge and exciton distribution towards extremely high performance: The critical role of guests in single-emitting-layer white OLEDs. *Mater. Horiz.* **2015**, *2*, 536–544.
13. Ying, S.; Sun, Q.; Dai, Y.; Yang, D.; Qiao, X.; Ma, D. Precise regulation of the emissive layer for ultra-high performance white organic light-emitting diodes in an exciplex forming co-host system. *Mater. Chem. Front.* **2019**, *3*, 640–649. [[CrossRef](#)]
14. Liu, B.; Nie, H.; Zhou, X.; Hu, S.; Luo, D.; Gao, D.; Zou, J.; Xu, M.; Wang, L.; Zhang, Z.; et al. Manipulation of charge and exciton distribution based on blue aggregation-induced emission fluorophors: A novel concept to achieve high-performance hybrid white organic light-emitting diodes. *Adv. Funct. Mater.* **2016**, *26*, 776–783. [[CrossRef](#)]
15. Wu, S.F.; Li, S.H.; Wang, Y.K.; Huang, C.C.; Sun, Q.; Liang, J.J.; Liao, L.S.; Fung, M.K. White Organic LED with a Luminous Efficacy Exceeding 100 lm W⁻¹ without Light Out-Coupling Enhancement Techniques. *Adv. Funct. Mater.* **2017**, *27*, 1701314. [[CrossRef](#)]
16. Zhao, J.; Yuan, S.; Du, X.; Li, W.; Zheng, C.; Tao, S.; Zhang, X. White OLEDs with an EQE of 21% at 5000 cd m⁻² and ultra high color stability based on exciplex host. *Adv. Opt. Mater.* **2018**, *6*, 1800825. [[CrossRef](#)]
17. Ying, S.; Xiao, S.; Yao, J.; Sun, Q.; Dai, Y.; Yang, D.; Qiao, X.; Chen, J.; Zhu, T.; Ma, D. High-performance white organic light-emitting diodes with high efficiency, low efficiency roll-off, and superior color stability/color rendering index by strategic design of exciplex hosts. *Adv. Opt. Mater.* **2019**, *7*, 1901291. [[CrossRef](#)]
18. Sheng, R.; Li, A.; Zhang, F.; Song, J.; Duan, Y.; Chen, P. Highly efficient, simplified monochrome and white organic light-emitting devices based on novel exciplex host. *Adv. Opt. Mater.* **2020**, *8*, 1901247. [[CrossRef](#)]
19. Liu, X.; Yao, B.; Zhang, Z.; Zhao, X.; Zhang, B.; Wong, W.Y.; Cheng, Y.; Xie, Z. Power-efficient solution-processed red organic light-emitting diodes based on an exciplex host and a novel phosphorescent iridium complex. *J. Mater. Chem. C* **2016**, *4*, 5787–5794. [[CrossRef](#)]
20. Kim, K.H.; Yoo, S.J.; Kim, J.J. Boosting triplet harvest by reducing nonradiative transition of exciplex toward fluorescent organic light-emitting diodes with 100% internal quantum efficiency. *Chem. Mater.* **2016**, *28*, 1936–1941. [[CrossRef](#)]
21. Goushi, K.; Adachi, C. Efficient organic light-emitting diodes through up-conversion from triplet to singlet excited states of exciplexes. *Appl. Phys. Lett.* **2012**, *101*, 023306. [[CrossRef](#)]
22. Shin, H.; Lee, J.H.; Moon, C.K.; Huh, J.S.; Sim, B.; Kim, J.J. Sky-blue phosphorescent OLEDs with 34.1% external quantum efficiency using a low refractive index electron transporting layer. *Adv. Mater.* **2016**, *28*, 4920–4925. [[CrossRef](#)] [[PubMed](#)]

23. Yao, J.; Ying, S.; Qiao, X.; Yang, D.; Chen, J.; Ahamad, T.; Alshehri, S.M.; Ma, D. High efficiency and low roll-off all fluorescence white organic light-emitting diodes by the formation of interface exciplex. *Org. Electron.* **2019**, *67*, 72–78. [[CrossRef](#)]
24. Zhang, D.; Cai, M.; Zhang, Y.; Bin, Z.; Zhang, D.; Duan, L. Simultaneous enhancement of efficiency and stability of phosphorescent OLEDs based on efficient Förster energy transfer from interface exciplex. *ACS Appl. Mater. Interfaces* **2016**, *8*, 3825–3832. [[CrossRef](#)] [[PubMed](#)]
25. Wu, M.; Wang, Z.; Liu, Y.; Qi, Y.; Yu, J. Non-doped phosphorescent organic light-emitting devices with an exciplex forming planar structure for efficiency enhancement. *Dyes Pigment.* **2019**, *164*, 119–125. [[CrossRef](#)]
26. Wang, J.; Zhang, X.; Fan, L.; Zhang, X.; Qin, Y.; Li, R.; Chen, Y.; Lai, W.Y.; Zhang, X.; Huang, W. Highly efficient solution-processed red phosphorescent organic light-emitting diodes employing an interface exciplex host. *J. Mater. Chem. C* **2020**, *8*, 9909–9915. [[CrossRef](#)]
27. Shih, P.I.; Shu, C.F.; Tung, Y.L.; Chi, Y. Efficient white-light-emitting diodes based on poly (N-vinylcarbazole) doped with blue fluorescent and orange phosphorescent materials. *Appl. Phys. Lett.* **2006**, *88*, 251110. [[CrossRef](#)]
28. Hu, S.; Zeng, J.; Zhu, X.; Guo, J.; Chen, S.; Zhao, Z.; Tang, B.Z. Universal bipolar host materials for blue, green, and red phosphorescent OLEDs with excellent efficiencies and small-efficiency roll-off. *ACS Appl. Mater. Interfaces* **2019**, *11*, 27134–27144. [[CrossRef](#)]
29. Sheng, R.; Song, J.; Li, A.; Zhang, F.; Zhang, H.; Duan, Y.; Zheng, J.; Wang, Z.; Chen, P. High-efficiency and low efficiency roll-off in white organic light-emitting diodes employing a novel blue emitter. *Org. Electron.* **2019**, *75*, 105375. [[CrossRef](#)]
30. Song, J.; Zhang, F.; Yang, L.; Chen, K.; Li, A.; Sheng, R.; Duan, Y.; Cheng, P. Highly efficient, ultralow turn-on voltage red and white organic light-emitting devices based on a novel exciplex host. *Mate. Adv.* **2021**, *2*, 3677–3684. [[CrossRef](#)]
31. Sheng, R.; Zhang, E.; Zhao, W.; Chen, C.; Ma, W.; Shao, J.; Duan, Y.; Zhao, Y.; Chen, P. Engineering of interface exciplex system for highly efficient white organic light-emitting diodes based on single-emission-layer architecture. *Org. Electron.* **2022**, *100*, 106382. [[CrossRef](#)]
32. Jia, L.; Jin, L.; Yuan, K.; Chen, L.; Yuan, J.; Xu, S.; Lv, W.; Chen, R. High-performance exciplex-type host for multicolor phosphorescent organic light-emitting diodes with low turn-on voltages. *ACS Sustain. Chem. Eng.* **2018**, *6*, 8809–8815. [[CrossRef](#)]
33. Lee, S.; Kim, K.H.; Limbach, D.; Park, Y.S.; Kim, J.J. Low roll-off and high efficiency orange organic light emitting diodes with controlled co-doping of green and red phosphorescent dopants in an exciplex forming co-host. *Adv. Funct. Mater.* **2013**, *23*, 4105–4110. [[CrossRef](#)]
34. Gao, K.; Liu, K.; Li, X.L.; Cai, X.; Chen, D.; Xu, Z.; He, Z.; Li, B.; Qiao, Z.; Chen, D.; et al. An ‘Ideal’ Universal Host for Highly Efficient Full-Color, White Phosphorescent and Thermally Activated Delayed Fluorescent OLEDs with Extremely Simple and Unified Structure. *J. Mater. Chem. C* **2017**, *5*, 10406–10416. [[CrossRef](#)]
35. Sheng, R.; Yang, L.; Li, A.; Chen, K.; Zhang, F.; Duan, Y.; Zhao, Y.; Chen, P. Highly efficient orange and white OLEDs based on ultrathin phosphorescent emitters with double reverse intersystem crossing system. *J. Lumin.* **2022**, *246*, 118852. [[CrossRef](#)]
36. Tian, Q.S.; Zhang, L.; Hu, Y.; Yuan, S.; Wang, Q.; Liao, L.S. High-performance white organic light-emitting diodes with simplified structure incorporating novel exciplex-forming host. *ACS Appl. Mater. Interfaces* **2018**, *10*, 39116–39123. [[CrossRef](#)]
37. Yu, Z.; Feng, H.; Zhang, J.; Liu, S.; Zhao, Y.; Zhang, L.; Xie, W. Carrier transport manipulation for efficiency enhancement in blue phosphorescent organic light-emitting devices with a 4, 4'-bis (N-carbazolyl)-2, 2'-biphenyl host. *J. Mater. Chem. C* **2019**, *7*, 9301–9307. [[CrossRef](#)]
38. Chen, C.; Liu, Y.F.; Chen, Z.; Wang, H.R.; Wei, M.Z.; Bao, C.; Zhang, G.; Gao, Y.H.; Liu, C.L.; Jiang, W.L.; et al. High efficiency warm white phosphorescent organic light emitting devices based on blue light emission from a bipolar mixed-host. *Org. Electron.* **2017**, *45*, 273–278. [[CrossRef](#)]
39. Lee, J.H.; Cheng, S.H.; Yoo, S.J.; Shin, H.; Chang, J.H.; Wu, C.I.; Wong, K.T.; Kim, J.J. An exciplex forming host for highly efficient blue organic light emitting diodes with low driving voltage. *Adv. Funct. Mater.* **2015**, *45*, 361–366. [[CrossRef](#)]

Disclaimer/Publisher’s Note: The statements, opinions and data contained in all publications are solely those of the individual author(s) and contributor(s) and not of MDPI and/or the editor(s). MDPI and/or the editor(s) disclaim responsibility for any injury to people or property resulting from any ideas, methods, instructions or products referred to in the content.